

# Resistance of poly(lactic acid)/starch composites to weathering effects

Victoria Goetjes  | Jan-Christoph Zarges | Hans-Peter Heim

Institute of Material Engineering, Polymer Engineering, University of Kassel, Kassel, Germany

## Correspondence

Victoria Goetjes, Institute of Material Engineering, Polymer Engineering, University of Kassel, Mönchebergstr. 3, 34125 Kassel, Germany.  
Email: [victoria.goetjes@uni-kassel.de](mailto:victoria.goetjes@uni-kassel.de)

## Funding information

the Federal Ministry of Food and Agriculture; the Fachagentur Nachwachsende Rohstoffe e.V.

## Abstract

In order to produce a completely bio-based and cost-effective filled polymer, PLA and native potato starch as a filler were compounded by twin screw extrusion. Subsequently injection molded test specimens were manufactured and subjected to artificial weathering as well as different storages (high temperature, high humidity, freeze, water) for 504 h with a view to long-term resistance. Depending on the starch content a significant reduction of up to 100% in tensile strength can be seen, as the starch accelerates or inhibits the triggered aging effects. As a result of the influence of humidity and water as well as artificial weathering, stress cracks are formed in starch-containing samples. Storage at an elevated temperature (70°C, 50% RH) leads to polymer degradation of the PLA. This degradation can be inhibited by the addition of starch. Freezing storage has no significant influence on the mechanical and structural properties of the PLA starch composites.

## KEYWORDS

aging, biopolymers, durability, hydrolysis, PLA, starch

## 1 | INTRODUCTION

Poly(lactic acid) (PLA) is one of the most important bioplastics on the global market and accounts for 20.5% of the total amount of bioplastics produced annually.<sup>1</sup> Despite good mechanical properties and high availability, the use is inhibited by the high price compared to polyolefins. One way to solve this problem is to add low-cost fillers such as native starch.<sup>2</sup> The use of starch is accompanied by a change in the mechanical, thermal, and structural properties, but also leads to an improvement in the carbon footprint.<sup>3</sup> By saving PLA, not only costs can be reduced, but also the energy that must be expended for the synthesis. Starch, on the other hand, already binds CO<sub>2</sub> during the plant growth phase.<sup>2,4</sup> Composites of starch types from different origins have already been produced. In addition to potato starch, rice, tapioca and corn starch were also

used.<sup>5–18</sup> The addition of native starch to a PLA matrix leads to an embrittlement and thus a decrease in tensile strength and elongation at break, with an increasing effect with rising starch content.<sup>3,13</sup> Due to their properties, PLA starch composites are suitable for a wide range of applications, which are currently mainly limited to plastic trays, loose-fills, cutlery, and writing instruments.<sup>2,19</sup>

During use, components are exposed to numerous environmental influences such as temperature, humidity, and UV radiation. These influences, in turn, cause complex aging phenomena, which become noticeable in the properties of the composites. In particular, starch can increase the causes of aging such as water absorption, and therefore promote aging processes.<sup>20</sup> This is based on the polar groups of the starch, which lead to hydrogen bondings and thus form the strongly hydrophilic character of starch.<sup>2</sup> For PLA, which is known to be a material

This is an open access article under the terms of the [Creative Commons Attribution](https://creativecommons.org/licenses/by/4.0/) License, which permits use, distribution and reproduction in any medium, provided the original work is properly cited.

© 2023 The Authors. *Journal of Applied Polymer Science* published by Wiley Periodicals LLC.

prone to hydrolysis, the increased water absorption is accompanied by a change in properties.<sup>21–25</sup> In 2003, Wang et al.<sup>26</sup> investigated the physical aging of composites of PLA and starch and observed a deterioration of the mechanical properties as a result of storage at 25°C and 50% humidity. In addition, the microstructure of the composites also changed and showed an increasing ductility of the matrix with continued physical aging and a simultaneous deterioration of the bond between the starch and the matrix, which in turn caused a decrease in tensile strength. Yew et al.<sup>27</sup> and Gáspár et al.<sup>28</sup> also showed a reduction in mechanical properties as a result of humid storage. Yew et al.<sup>27</sup> showed a clearly stronger and accelerated water absorption of PLA through the addition of hygroscopic starch, whereby the samples with 20% starch absorbed 5 times as much water as pure PLA samples. It is assumed that the absorbed water leads on the one hand to hydrolysis of the PLA and on the other hand to a deterioration of the adhesion between PLA and starch and thus to a reduction in the mechanical properties. Similarly, artificial weathering of PLA starch composites led to a reduction in tensile strength, although the reduction was less for starch-containing samples than for pure PLA. The reason for this is the UV-shielding effect of the starch particles, which slows down the UV-induced chain degradation.<sup>6</sup> In addition to starch-filled PLA, there are also numerous studies on LDPE that have been filled with starch: Danjaji et al.<sup>29</sup> showed a decrease in the tensile strength of starch-filled LLDPE as a result of significantly increased water absorption. Furthermore, the thermal degradation of LDPE can be inhibited by the addition of starch.<sup>30</sup>

Previous studies have made it clear that the addition of starch on the one hand increases water absorption and can thus reduce the mechanical properties of starch composites, but on the other hand, can also slow down degradation reactions. However, there is insufficient knowledge about the exact degradation mechanisms of PLA potato starch composites that are triggered by various and, in particular, combined environmental influences.

The aim of this work is therefore to carry out comprehensive investigations regarding the influence of environmental conditions on the properties of PLA starch composites with potato starch and in consequence expand the areas of application. For this purpose, composites with two different starch contents were subjected to different environmental storage conditions in order to initiate aging processes in them. Composites of PLA with 40 wt.% and 50 wt.% potato starch were produced, processed into test specimens, and aged under the

influence of varying environmental conditions. Subsequently, the properties of the aged composites were characterized mechanically, structurally, and optically, with a particular focus on the developing crack paths.

## 2 | MATERIALS AND METHODS

### 2.1 | PLA and potato starch

PLA Luminy® L130 provided by TotalEnergies Corbion (NS Gorinchem, Netherlands) was used for the investigations. It is a semi-crystalline type, which therefore has a higher temperature resistance than comparable PLA types. The density is 1.24 g/cm<sup>3</sup> and the melting temperature is 175°C.

Native potato starch type Superior from the company Emsland Stärke (Emlichheim, Germany) was used as filler. In order to assess the influence of the filler on the blend properties, test specimen of unfilled PLA was investigated for reference purposes to the specimen of PLA filled with 40 and 50 wt% starch.

### 2.2 | Preparation of the composites

The PLA starch composites were compounded using a ZSE 18 HPe twin-screw extruder (Leistritz Extrusionstechnik GmbH, Nuremberg, Germany) with a screw diameter of 18 mm and a process length of 40 D. Both PLA and starch were pre-dried before processing. For the PLA, a temperature of 100°C was used in a Dry Jet Easy compressed air oven (TORO-Systems, Igensdorf, Germany) for 6 h, while the starch was dried in a convection oven at 105°C for also 6 h.<sup>3</sup> The PLA was fed to the extruder via the main feeding section and melted up to the third zone, where kneading elements are located. In zone 4, starch was added and mixed with the PLA melt through mixing elements in zones 6 and 7, followed by degassing in zone 7. A throughput of 3 kg/h was achieved at a screw speed of 200 rpm. To avoid (thermal) damage of the starch, a gentle screw configuration and low temperatures were used.<sup>3</sup> The used screw and temperature profile are shown in Figure 1.

### 2.3 | Injection molding

The test specimens of type 1A according to DIN EN ISO 527-2 were produced with a hydraulic injection molding

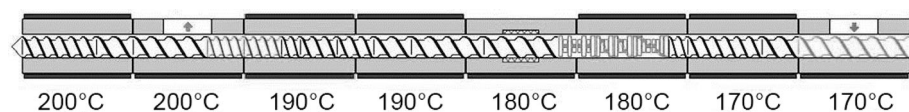


FIGURE 1 Temperature profile and screw configuration of the twin-screw extruder.

machine Allrounder 320C (Arburg GmbH + Co. KG, Lossburg, Germany). Test specimens were produced from pure PLA and from 40 wt% and 50 wt.% starch-filled PLA. To prevent hydrolytic degradation of the material during processing, the PLA and the composites were dried at 100°C for 6 h. The cycle time was approx. 98 s, while the maximum injection pressure was 1040 bar (filled material). The subsequent holding pressure was carried out with a pressure drop from 700 bar to 500 bar at a time of 25 s. The set temperatures are shown in Table 1.

## 2.4 | Environmental influences and artificial weathering

In order to investigate the influence of different environmental conditions on the properties of the composites, both unfilled test specimens made of pure PLA and filled with 40 wt.% and 50 wt.% starch were exposed to environmental influences for 504 h each. Reference samples from each material were stored in the standard climate (S) according to DIN EN ISO 291 at 23°C and 50% RH. In addition, aging took place at elevated humidity (H) at 23°C and 90% RH, at elevated temperature (T) at 70°C and 50% RH, as well as in a water bath (W) at a temperature of 23°C and freezing at -18°C (F).

In addition, the test specimens were subjected to 504 h of cyclical artificial weathering (WE) to simulate outdoor use. Both the 18-hour summer and winter cycles, shown in Figure 2, were repeated 14 times each.

Following all aging processes of 504 h each, the test specimens were conditioned for 168 h in a standard climate (23°C, 50% RH) prior to their testing and characterization.

## 2.5 | Differential scanning calorimetry

DSC analysis was used to determine the degree of crystallinity of the unaged test specimens in order to make predictions about their durability. The DSC module Q2000 f (TA Instruments, New Castle, USA) was used for the investigations. At a heating rate of 10°C/min, the test specimens were heated from 0°C to 250°C. The crystallinity of the PLA was determined using the enthalpy of fusion ( $\Delta H_f$ ), the enthalpy of crystallization ( $\Delta H_c$ ), the 100% crystallinity value of PLA of 93.6 J/g ( $\Delta H_f^0$ ), and the mass fraction of the matrix ( $w$ ),<sup>6,31,32</sup> shown in equation 1.

$$X_c[\%] = \frac{\Delta H_f - \Delta H_c}{w \cdot \Delta H_f^0} \cdot 100, \quad (1)$$

TABLE 1 Temperature profile of the injection molding process.

Zone	1	2	3	4	5	Nozzle	Mold temperature
Temperature in °C	200	205	210	215	215	215	30

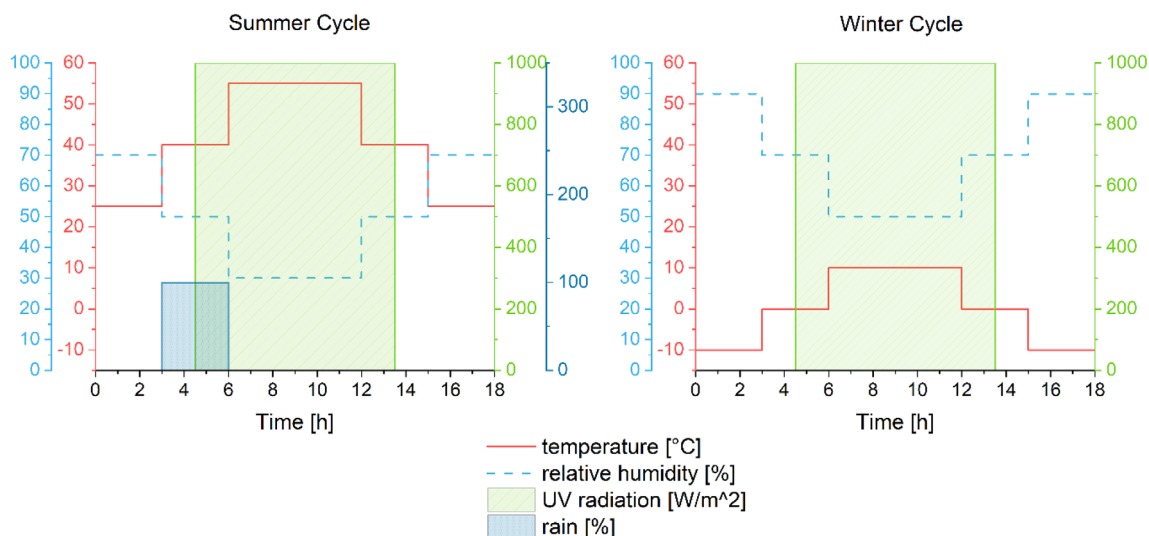


FIGURE 2 Artificial weathering (WE) consisting of 14 summer cycles and 14 winter cycles. [Color figure can be viewed at [wileyonlinelibrary.com](http://wileyonlinelibrary.com)]

## 2.6 | Tensile test

The aged and conditioned specimens were subjected to a tensile test according to DIN EN ISO 527 on a UPM 1446 testing machine (Zwick Roell, Ulm, Germany). Five test specimens were tested per batch at a test speed of 5 mm/min and the Young's modulus, the tensile strength as well as the elongation at break were determined. The significance was determined using a t-test at a significance level of 0.05.

## 2.7 | Scanning electron microscopy

The fracture surfaces of the specimens from the tensile test were characterized using an MV2300 scanning electron microscope (SEM) from CamScan Electron Optics Services (Ottawa, Canada), using only the unfilled specimens and those filled with 50 wt.% starch. A 50 $\times$ , a 500 $\times$ , and a 1500 $\times$  magnification used at an accelerating voltage of 10 kV were used for the investigations. An investigation of the sample surface did not take place and can therefore not be excluded.

## 2.8 | X-ray microtomography analysis ( $\mu$ CT)

In addition to the SEM analysis of the fracture surface, the samples were examined with the aid of X-ray Microtomography Analysis. Therefore, an Xradia Versa 520 (Carl Zeiss, Oberkochen, Germany) was used in order to make statements about the crack paths inside the sample. For this purpose, cube-shaped specimens with an edge length of 4 mm were sawed out of the center of the shoulder bars from the aged tensile test specimen.

The measurements were carried out at a voltage of 60 kV and a current of 83.3  $\mu$ A using the LE1 filter and a 4x objective. The voxel size was 1.55  $\mu$ m and the exposure time was 6 s for each image. The reconstruction was done using the Zeiss XMReconstructor software.

## 2.9 | Particle measurement

The size distribution of dried and wet native potato starch particles was analyzed using the dynamic image analysis system QicPic (Sympatech, Clausthal-Zellerfeld, Germany). Dried starch was dehydrated at 105 $^{\circ}$ C for 6 h as before processing. The wet starch was stored at water bath at 23 $^{\circ}$ C for 1, 2, or 4 h. The starch was fed to the QicPic via the liquid dispersion unit MIXCEL with the carrier medium water through an 0.5 mm cuvette past a high-speed camera

(M4 lens) and recorded at a frequency of 175 Hz. The subsequent evaluation via Sympatech's WINDOX software provides insights into the particle shape and mean particle size as well as their distribution.

## 2.10 | Humidity absorption of aged samples

To determine the humidity absorption ( $\omega$ ) of the samples as a result of aging, the weight of each sample was determined before ( $m_S$ ) and after aging ( $m_X$ ) and the increase in humidity content was calculated according to DIN EN 13183-1, shown in Equation 2.

$$\omega[\%] = \frac{m_X - m_S}{m_S} \cdot 100, \quad (2)$$

## 2.11 | Gel permeation chromatography

In order to identify chemical aging as a result of exposure to environmental influences on filled and unfilled PLA, GPC analysis were performed. The measurement was carried out at the Fraunhofer-Institute for Applied Polymer Research (Potsdam-Golm, Germany) according to DIN 55672-1. The eluent used was Trichlormethan (TCM) at 25 $^{\circ}$ C.

The number average molecular weight ( $M_n$ ), weight average molecular weight ( $M_w$ ), and molecular weight distributions were determined for all test samples.

# 3 | RESULTS AND DISCUSSION

## 3.1 | Prediction of resistance of composites via differential scanning calorimetry

With the use of the DSC measurements, the crystallinity of the unaged material can be determined. As increased crystallinity is expected to increase resistance, the unaged test specimens were subjected to a DSC<sup>6</sup> whereby the calculated crystallinities are shown in Table 2. With 15.0%,

TABLE 2 Calculated crystallinity of unaged, filled, and unfilled PLA.

Mass fraction starch in %	X <sub>c</sub> in %
0	15,0
40	40,2
50	78,5

the unfilled samples show the lowest crystallinity. The addition of starch as a filler leads to a significant increase in crystallinity to 40.2% (40 wt.% starch) and 78.5% (50 wt.% starch). An increase in crystallinity for starch filled PLA was also observed in various investigations.<sup>3,6,7,17</sup> It can be concluded, that starch acts as a nucleating agent for PLA. Accordingly, it can be suggested that the starch-containing samples show better resistance than the pure PLA samples.

### 3.2 | Effect of environmental influences on mechanical properties

The tensile strength as a function of the starch content is shown in Figure 3. With increasing starch content, the tensile strength decreases for the unaged and aged samples. The pure PLA samples (0 wt.% starch) show no significant decrease in tensile strength due to aging in freeze (F), humidity (H) and water storage (W). Weathered (WE) or temperature-stored (T) samples on the other hand show a significant reduction in tensile strength. Compared to the temperature-stored PLA samples, the weathered PLA samples have a significant increase in tensile strength of 9.5%, while the temperature-stored PLA samples are severely damaged.

For the starch-containing samples, a significant reduction in tensile strength is observed through all ageings except freeze. Compared to the reference samples (S) with 40 and 50 wt.% starch, the humidity (H) and water stored (w) samples show the strongest reduction in tensile strength, with a decrease of 45.6% (H) and 43.9% (W), respectively, at 40 wt.% starch and 52.1% (H) and 60.8% (W) at 50 wt.% starch. The weathered (WE) and filled samples, which were exposed to a cyclic load of varying humidity, temperature, and UV radiation, show a slightly but significantly lower

reduction of 30.3% (40 wt.%) and 25.9% (50 wt.%). Yew et al.<sup>27</sup> and Gáspár et al.<sup>28</sup> also observed a reduced tensile strength for starch containing samples after humid or wet storage and related this to hydrolytic degradation. Since the decrease in tensile strength only occurs for the starch-containing samples, it can be assumed that there is no hydrolytic degradation and the starch is causal for the water-induced changes in the material properties, which can be described as physical aging. A possible reason could be the swelling effects of the hydrophilic starch particles, which damage the surrounding matrix, as is already known for the use of various natural fibers.<sup>33–37</sup> This swelling effect could also lead to damage for the weathered samples, whereby it can be assumed that a minor cross-linking of the PLA matrix by the UV radiation takes place simultaneously, as it was also observed by Lv, Gu et al.<sup>6</sup> DSC analysis would suggest improved resistance for the starch-containing samples due to increased crystallinity. However, since the reduced mechanical properties can be attributed to physical damage caused by swelling starch, crystallinity cannot have a significant effect on resistance to humidity and water-induced physical aging.

The test specimens that were stored for 504 h at elevated temperature were so severely damaged due to the aging that they could not be subjected to a tensile test. In order to nevertheless be able to evaluate the effect of temperature storage, test specimens were taken after 168 h of aging and tested accordingly, although it should be noted that they are not comparable with 504 h of aging. The temperature stored (T) samples show a different relationship between tensile strength and starch content compared to other ageings. Both unfilled and filled samples show significantly reduced tensile strength (100% for unfilled PLA; 87.9% for 40 wt.% starch; 85.5% for 50 wt.% starch), which

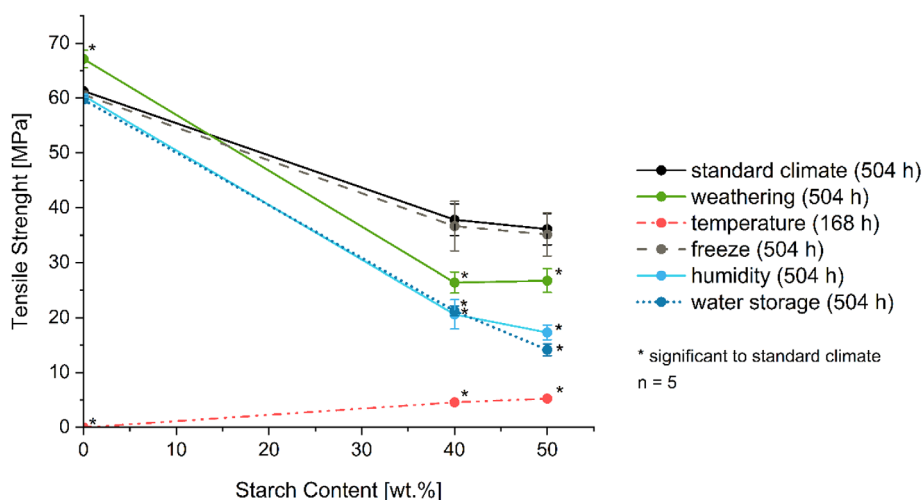


FIGURE 3 Tensile strength of the aged starch filled and unfilled samples as a function of starch content and aging (\* - significant change in tensile strength compared with reference (S)).

[Color figure can be viewed at [wileyonlinelibrary.com](http://wileyonlinelibrary.com)]

increases with increasing starch content. The effect expected from DSC, that is, improved durability with the addition of a nucleating filler such as starch, was found. Since a significant reduction of the tensile strengths, especially for the pure PLA sample, is nevertheless observed as a result of the temperature storage, it can be assumed that a degradation of the polymer has taken place. Both Hydrolysis<sup>22,38–47</sup> and thermal-oxidative degradation<sup>38</sup> can be considered.

The characterizations carried out in addition were intended to test the hypotheses made and so find the causes for the aging-related changes in the mechanical properties.

### 3.3 | Fracture surface

The analysis of the fracture surface with the aid of the scanning electron microscope provides insights into the bonding between starch particles and PLA, as well as failure mechanisms. Figure 4 shows exemplary images of the fracture surfaces (test specimen centre) of unfilled PLA specimens (a), (c), (e) and specimens filled with 50 wt.% starch (b), (d), (f) as a function of aging (reference (S) – (a), (b)), humidity (H) – (c), (d)), temperature (T) – (e), (f)). For the filled standard climate sample (b) a clear demarcation between starch particles and PLA can be observed, as also observed by Yew et al.<sup>27</sup> There is no

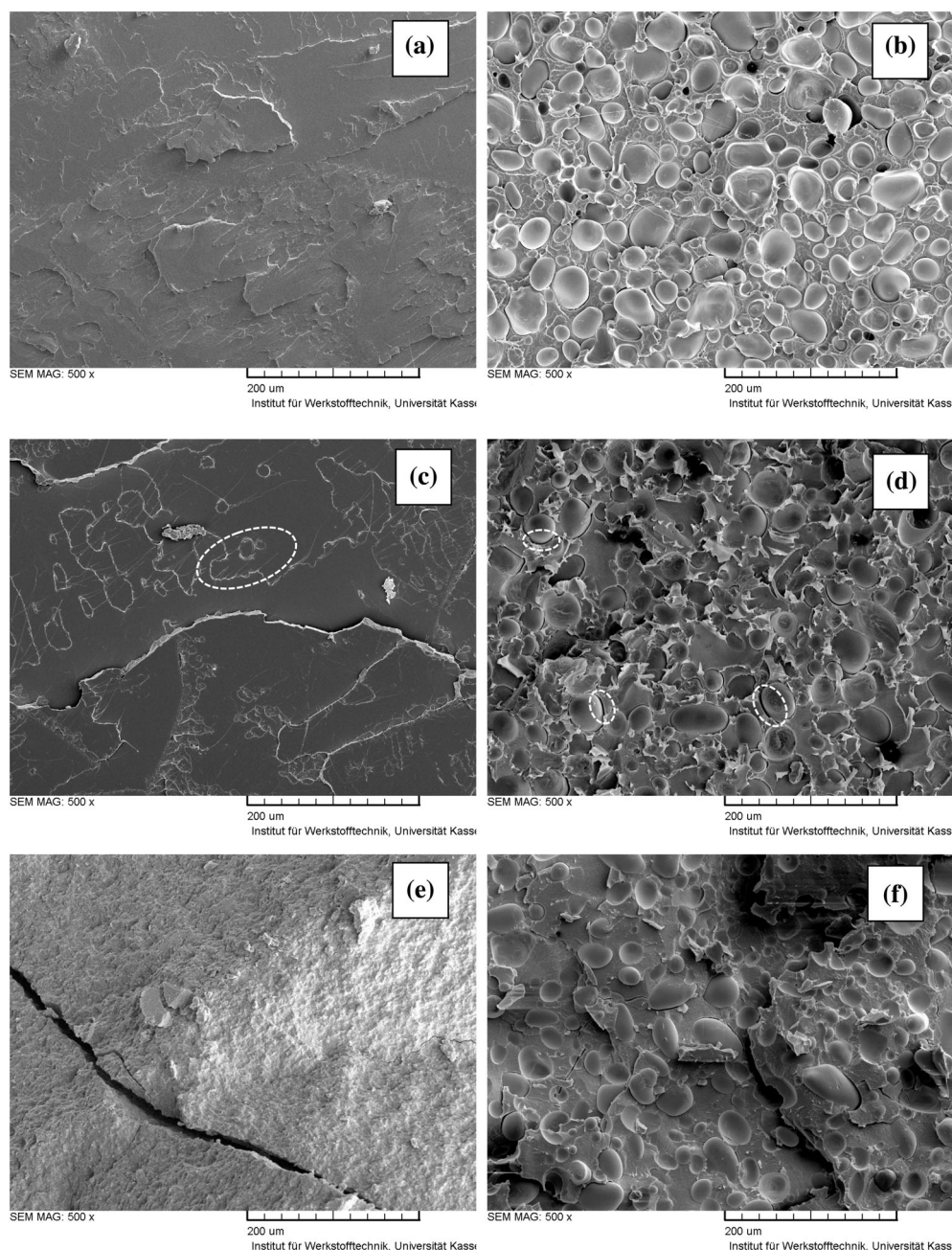


**FIGURE 4** SEM images (magnification 500×) of aged unfilled and starch filled (50 wt.%) PLA fracture surfaces: (a) unfilled PLA after standard climate (s); (b) PLA starch composite after standard climate (S); (c) unfilled PLA after humidity (H); (d) PLA starch composite after humidity (H); (e) unfilled PLA after temperature (t); (f) PLA starch composite after temperature (T).

residue of the matrix on the starch particles, which indicates insufficient bonding. Due to the influence of humidity, only a slightly increased ductile behavior can be observed in the pure PLA sample (c) compared to standard PLA (a), which is noticeable in the formation of narrow threads.<sup>27</sup> For the filled sample (d), on the other hand, some large gaps between starch particles and the matrix can be identified. The number and size of the gaps increase significantly in the near surface regions of the sample. Furthermore, a more ductile material behavior of the matrix can be concluded due to the torn out matrix surface. These observations were also made for the water-stored samples. Both the unfilled (e) and the filled (f) sample show clear crack paths in the entire cross-sectional area of the sample after temperature storage. The pure sample (e) also shows a very rough fracture surface.

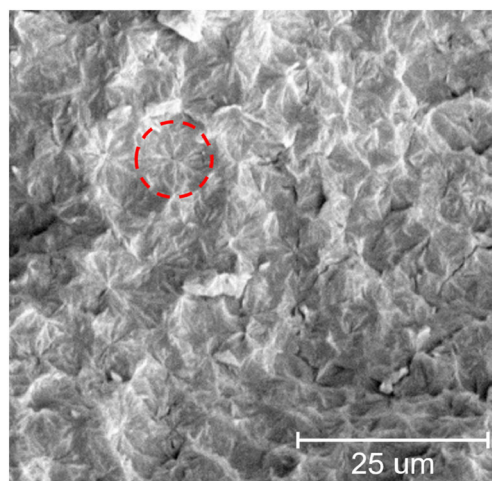
Considering water-aged samples, shown in Figure 5, the clear formation of cracks, which are already wide open (b), in the surface near area is noticeable (c). Especially in this edge area, very large gaps between starch particles and PLA matrix can be observed (a). The gaps between starch and PLA remaining after water and humidity storage speak for the presumed swelling effects of the starch particles. Gemmeke et al.,<sup>48</sup> Kahl et al.<sup>49</sup> and Falkenreck et al.<sup>50</sup> observed similar effects when using cellulose fibers in a thermoplastic matrix and also showed a reduced tensile strength. In addition, the also by Yew et al.<sup>27</sup> observed more ductile behavior of the matrix can be seen as a result of the influence of water (b).

Figure 6 shows the 1500 $\times$  magnification of the fracture surface of the temperature-aged PLA sample. It can be seen that the mentioned structural change of the fracture surface (compared to the standard sample) is due to the formation of spherulites, whereby the cracks often propagate along the spherulite boundaries. The

formation of a spherulitic structure can be an indication of degradation as a result of hydrolysis and therefore supports the hypothesis of polymer degradation.<sup>39</sup>

### 3.4 | X-ray microtomography analysis ( $\mu$ CT)

In order to evaluate the crack structure also in mechanically unloaded test specimens, X-ray Microtomography images of the filled specimens were taken. Figure 7 shows cross-sectional images of the test specimens in the middle of the test area of the shoulder bars. For reference specimen (a), which were stored in a standard climate, a homogeneous distribution of starch particles and no cracks can be seen. Both humidity- and water-stored



**FIGURE 6** SEM image (magnification 1500 $\times$ ) of aged unfilled PLA fracture surfaces after temperature (T). [Color figure can be viewed at [wileyonlinelibrary.com](http://wileyonlinelibrary.com)]

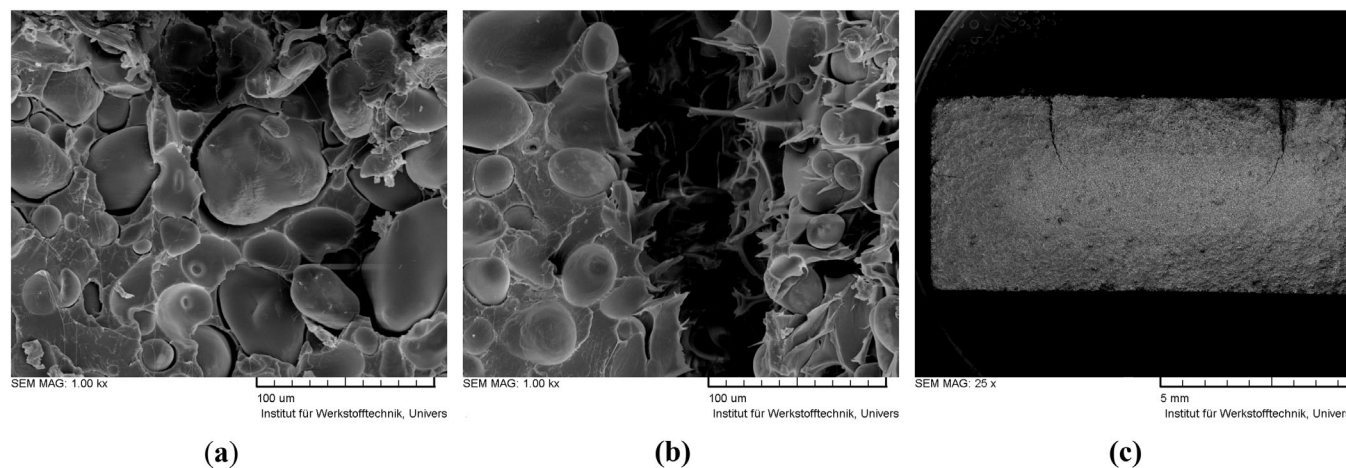


**FIGURE 5** SEM images of aged, starch filled (50 wt.%) PLA fracture surfaces after water storage (W): (a) edge area (magnification 1000); (b) crack structure in edge area (magnification 1000); (c) crack structure overview (magnification 25).

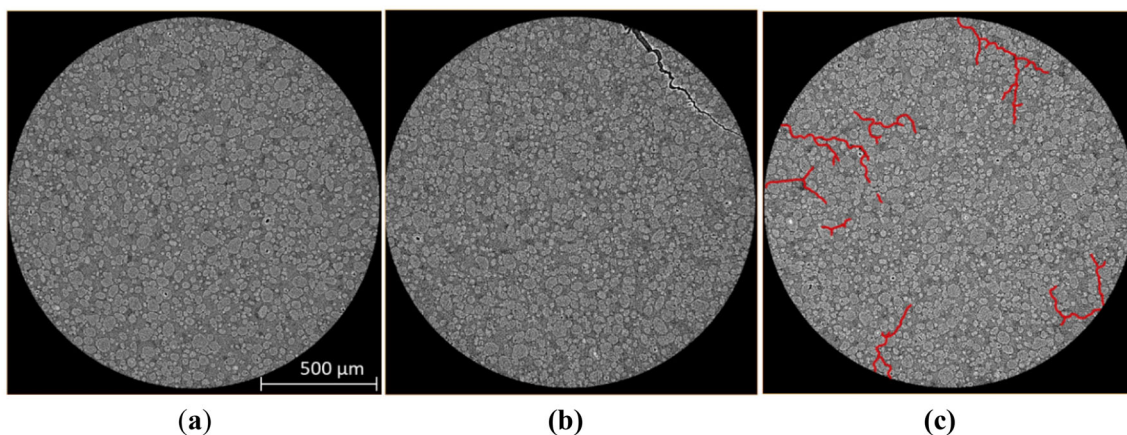


**FIGURE 7**  $\mu$ CT-images of aged, starch filled (50 wt.%) PLA: (a) PLA starch composite after standard climate (S); (b) PLA starch composite after humidity (H); (c) PLA starch composite after temperature (T). [Color figure can be viewed at [wileyonlinelibrary.com](http://wileyonlinelibrary.com)]

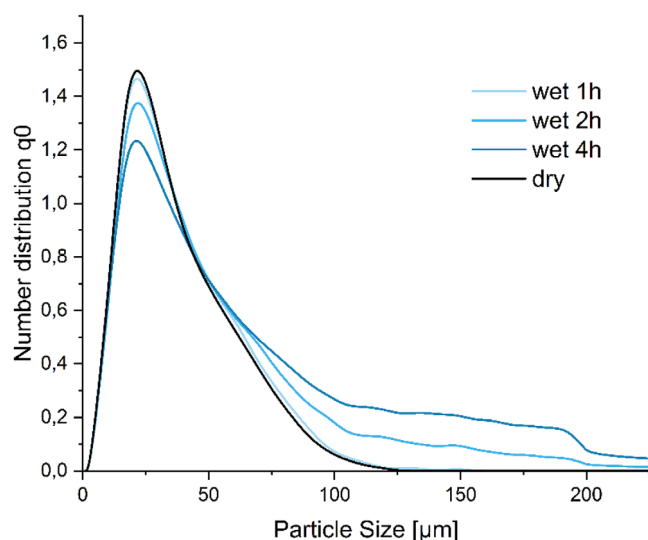


**FIGURE 8** Particle number distribution of dry and wet (1 h, 2 h, and 4 h) native potato starch. [Color figure can be viewed at [wileyonlinelibrary.com](http://wileyonlinelibrary.com)]

(b) samples show a clear crack structure in the edge area. These cracks propagate through the entire edge area of the sample where water could penetrate the most or the fastest, as Yew et al.<sup>27</sup> already observed. This observation also clearly speaks for the swelling effects of the starch particles, which increase their volume by absorbing water or humidity and introducing tension into the matrix. The one-week conditioning in the standard climate following storage causes the starch to release humidity or water again, reduces its volume, and leaves gaping cracks like the ones seen here. Since the water can penetrate better and faster in the edge area, cracks are found especially in this area.<sup>27</sup> In comparison, the temperature-aged samples (c) show a much finer crack structure, which not only extends to the edge area but runs through the entire test

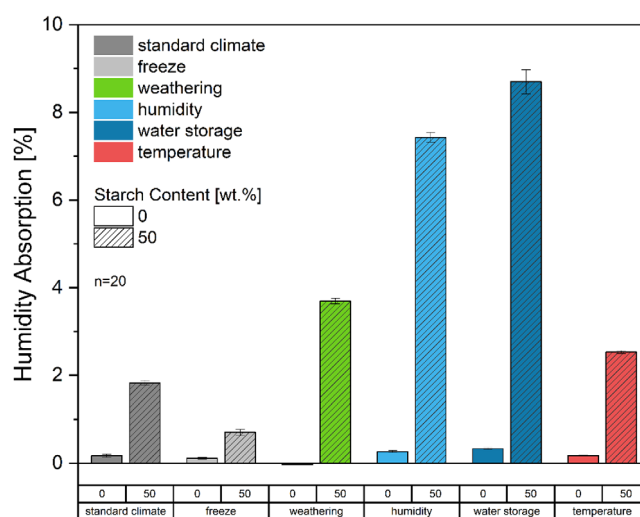


**FIGURE 9** Humidity absorption of the aged starch filled and unfilled samples. [Color figure can be viewed at [wileyonlinelibrary.com](http://wileyonlinelibrary.com)]

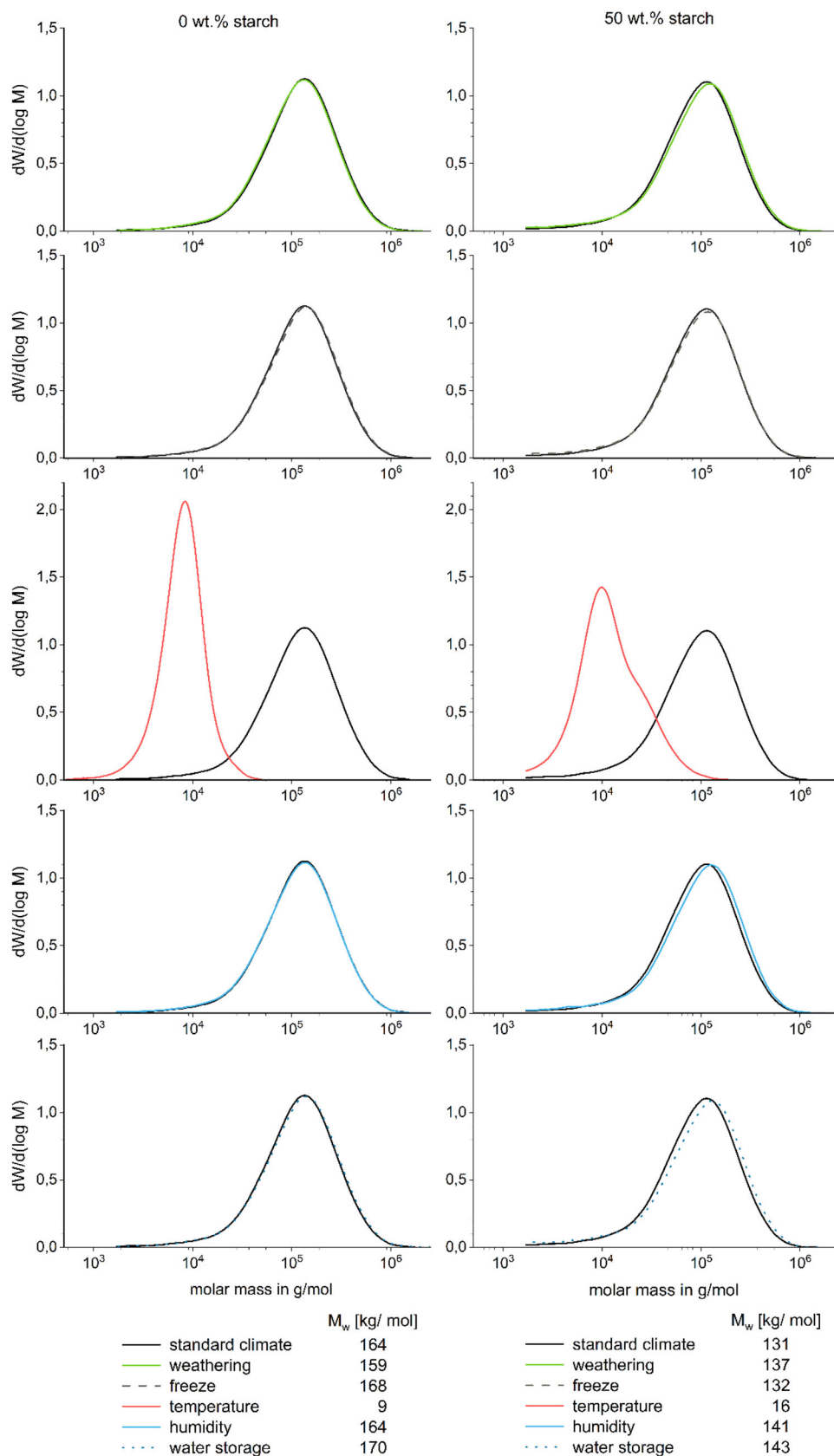
specimen. The cracks are colored red for better visibility. The developed crack paths, which are also present in the sample centre, indicate a degradation of the polymer and so go hand in hand with the results of the tensile test and the SEM images.<sup>51</sup> For all cracks, it is noticeable that they propagate along the interfaces between starch particles and PLA matrix, which indicates a low adhesion between starch and PLA, as observed in SEM pictures.

### 3.5 | Particle and humidity measurements

To investigate the physical behavior of native potato starch under the influence of water, both dried and wet



**FIGURE 10** Molar mass of unfilled and filled (50 wt% starch) PLA samples after 504 h aging. [Color figure can be viewed at [wileyonlinelibrary.com](http://wileyonlinelibrary.com)]



starch (water bath, 23°C) were measured. The measurement should provide information on whether the influence of water leads to swelling and the change in the

volume of starch particles. Figure 8 shows the number distribution of the particle size of the starch. With increasing storage time in the water bath, the size of

starch particles increases. There are fewer particles smaller than 50  $\mu\text{m}$  and more particles bigger than 50  $\mu\text{m}$  after 2 and 4 h. The reason for this is the swelling effect of the starch particles, which increase their volume under the influence of water or humidity.<sup>3,51–54</sup> The diffusion of water and humidity into the composite can therefore be assumed to cause swelling of the starch, which in turn creates tension in the surrounding matrix, which ultimately leads to failure or formation of cracks.<sup>51</sup>

In addition, the humidity content of the samples before and after aging was analyzed to detect an increased humidity content, especially in filled humidity and water storage samples. Figure 9 shows the increase in humidity of the samples because of aging. All filled samples show significantly higher humidity absorption than the identically stored unfilled samples. It can therefore be concluded that almost all the humidity is absorbed by the starch particles.

The lowest humidity uptake of the filled samples is shown by the freeze samples, as they do not have any humidity available to be absorbed. In the standard climate (50% RH) the filled samples absorb 1.8% moisture, during temperature storage (50% RH) 2.5%. This is due to the higher absolute humidity due to the increased temperature. Weathering leads to an increase in humidity of 3.7% for the filled samples. As a result of humidity and water storage, the highest increase of 7.4% (H) and 8.7% (W) can be observed.

### 3.6 | GPC

GPC analyses were carried out to identify possible degradation processes triggered by aging. Figure 10 shows the average molecular weight distribution of the unfilled and aged test specimens. The molar mass distribution does not change after 504 h of aging. Only for the temperature-aged samples, a strong significant reduction of the mean molar mass from 164 kg/mol (S) to 9 kg/mol (T) can be observed. Furthermore, the distribution becomes more homogeneous, that is, the width of the distribution decreases can be seen that degradation of the PLA takes place due to the temperature storage, which can be attributed to hydrolysis with the previous findings, especially from the SEM images.<sup>39</sup>

Looking at the molar mass distribution of the PLA matrix of the starch-containing samples (50 wt%), shown in Figure 10, very similar correlations can be seen. Only the temperature-aged samples show a significantly lower mean molar mass than the other aged, filled samples, with a reduction of 87.8% compared to the standard climate sample which is due to the hydrolytic degradation of the PLA. For the unfilled sample, on the other hand,

there is a greater reduction of 94.5% in the mean molar mass. Furthermore, all filled samples, except for the temperature aged sample, show a lower mean molar mass compared to the identically aged unfilled samples. This decrease in molecular weight is caused by the additional processing step of compounding.

## 4 | CONCLUSION

In the course of the work carried out, two fundamental influencing factors on the properties of the starch-filled and unfilled PLA can be identified. Storage at elevated humidity (H) or in a water bath (W) leads to a significant decrease in tensile strength for starch-filled samples, as also observed by Yew et al.<sup>27</sup> and Gáspár et al.<sup>28</sup> The water penetrating the sample does not trigger any degradation processes and so no decrease in the molar mass of the matrix material. Consequently, the change in the mechanical properties of the filled samples is due to the starch. The particle measurements show an increase in particle size and the well-known swelling behavior of starch.<sup>3,52</sup> This swelling in turn leads to the formation of the crack structure, which was observed both in the  $\mu\text{CT}$  and in the SEM. The formation of such cracks as a result of swelling and shrinkage effects and the resulting stresses is already known for numerous polymers.<sup>51</sup> The conditioning of the test specimens in a standard climate following storage results in a decrease in humidity and thus shrinkage of the starch particles. If the swelling and the resulting stresses are too great, stress cracks appear in the matrix. Due to the greater influence of humidity/water in the specimens edge area, cracks appear especially in the edge structure.

Storage of the unfilled and filled specimens at elevated temperature (T) also leads to a significant reduction of the tensile strength up to complete damage of the test specimens, whereby the damage decreases with increasing starch content. At this point, it can be concluded that the aging-related changes in matrix material are the cause of this change. The GPC investigations show a clear degradation of the PLA as a result of temperature storage. Two mechanisms known for PLA can be considered for the degradation: Hydrolysis<sup>22,38–47</sup> and thermal-oxidative degradation.<sup>38</sup> Within the scope of the conducted SEM analyses, the formation of spherulites can be observed after temperature storage, which can suggest a hydrolytic degradation of the PLA.<sup>39</sup> As a result of this degradation, an extensive crack structure is formed, which can be observed in the  $\mu\text{CT}$  as well as in the SEM images. The increasing crystallinity of the PLA starch composites with increasing starch content highlights the nucleating effect of the filler. This increased

crystallinity is in turn accompanied by improved resistance, especially to hydrolysis, as hydrolytic reactions occur predominantly in amorphous regions.<sup>55</sup> Thus, the increased crystallinity provides an explanation for the reduced decrease in tensile strength of the starch-containing samples as a result of temperature storage.

The weathering (WE) of the test specimens represents a combination of different aging mechanisms, whereby no aging in the form of polymer degradation occurs. Instead, it can be assumed that the alternating effects of varying humidity and temperature as well as sprinkling and UV radiation lead to physical aging, which mainly manifests itself in the formation of stress cracks.<sup>51</sup> As a result of these cracks, the tensile strength is reduced. Similar to samples stored in humidity (H) and water (W), this effect only occurs for samples containing starch.

Storage in freeze (F) does not show any change in the mechanical properties of the samples, which is why it can be assumed that no aging processes were triggered within the loading period of 504 h.

Overall, physical aging processes are caused by humidity and water (swelling) through the addition of native starch to PLA. A chemical degradation of the PLA in the form of hydrolysis occurs at the temperature storage (T) and can be reduced by the addition of the starch which leads to a reduction in degradation processes on the one hand. On the other hand, it leads to the initiation of stress cracks in damp or wet environments due to its swelling and shrinkage behavior.

The investigations carried out show that the addition of 50 wt% starch to PLA is accompanied by a significant reduction in the mechanical properties. Nevertheless, the addition of starch can lead to an improvement in resistance to degradation processes such as hydrolysis and therefore make an important contribution to the use of these composites in durable applications. A prerequisite for this is hydrophobisation of the starch to avoid the effects of physical aging due to swelling of the starch.

## AUTHOR CONTRIBUTIONS

**Victoria Goetjes:** Conceptualization (lead); data curation (lead); formal analysis (lead); investigation (lead); methodology (lead); project administration (lead); visualization (lead); writing – original draft (lead). **Jan-Christoph Zarges:** Writing – review and editing (equal). **Hans-Peter Heim:** Funding acquisition (lead); writing – review and editing (equal).

## ACKNOWLEDGMENTS

The authors would like to thank the Fraunhofer-Institute for Applied Polymer Research IAP (Potsdam-Golm, Germany) for carrying out the Gel Permeation Chromatography and the companies Emsland Stärke,

TechnoCompound GmbH and TotalEnergies Corbion for providing the materials for this investigation. This research was funded by the Federal Ministry of Food and Agriculture (BMEL) and the Fachagentur Nachwachsende Rohstoffe e.V. (FNR). Open Access funding enabled and organized by Projekt DEAL.

## CONFLICT OF INTEREST STATEMENT

The authors declare no conflict of interest.

## DATA AVAILABILITY STATEMENT

The data presented in this study are available on request from the corresponding author.

## ORCID

Victoria Goetjes  <https://orcid.org/0009-0009-0929-1186>

## REFERENCES

- [1] IfBB - Institute for Bioplastics and Biocomposites, Biopolymers - Facts and Statistics 2021: Production capacities, processing routes, feedstock, land and water use 2021.
- [2] O. Türk, *Stoffliche Nutzung nachwachsender Rohstoffe: Grundlagen - Werkstoffe - Anwendungen; mit 128 Tabellen*, Springer Vieweg, Wiesbaden 2014.
- [3] J. Fuchs, *Blends aus Stärke und PLA*, Kassel University Press, Kassel 2018.
- [4] A. Vercalsteren, K. Boonen, *Life Cycle Assessment Study of Starch Products for the European Starch Industry Association (Starch Europe): sector study*, Flemish Institute for Technological Research, Belgium 2015.
- [5] H.-J. Endres, M. Mundersbach, H. Behnsen, S. Spierling, *Bio-kunststoffe unter dem Blickwinkel der Nachhaltigkeit und Kommunikation: Status quo, Möglichkeiten und Herausforderungen*, Springer Vieweg, Wiesbaden 2020.
- [6] S. Lv, J. Gu, H. Tan, Y. Zhang, *J. Cleaner Prod.* 2018, 203, 328.
- [7] E. Laredo, D. Newman, R. Pezzoli, A. J. Müller, A. Bello, *J. Polym. Sci., Part B: Polym. Phys.* 2016, 54, 680.
- [8] S. Lv, J. Gu, J. Cao, H. Tan, Y. Zhang, *Int. J. Biol. Macromol.* 2015, 74, 297.
- [9] J.-F. Zhang, X. Sun, *J. Appl. Polym. Sci.* 2004, 94, 1697.
- [10] J.-F. Zhang, X. Sun, *Biomacromolecules* 2004, 5, 1446.
- [11] S. Jacobsen, H. G. Fritz, *Polym. Eng. Sci.* 1996, 36, 2799.
- [12] T. Ke, S. X. Sun, P. Seib, *J. Appl. Polym. Sci.* 2003, 89, 3639.
- [13] T. Ke, X. Sun, *Cereal Chem. J.* 2000, 77, 761.
- [14] T. Ke, X. Sun, *J. Appl. Polym. Sci.* 2001, 81, 3069.
- [15] T. Ke, X. Sun, *Am. Soc. Agric. Eng.* 2001, 44, 945.
- [16] T. Ke, X. S. Sun, *J. Appl. Polym. Sci.* 2003, 88, 2947.
- [17] T. Ke, X. Sun, *J. Appl. Polym. Sci.* 2003, 89, 1203.
- [18] N. H. Yusoff, K. Pal, T. Narayanan, F. G. De Souza, *J. Mol. Struct.* 2021, 1232, 129954.
- [19] H. A. Pushpadass, G. S. Babu, R. W. Weber, M. A. Hanna, *Packag. Technol. Sci.* 2008, 21, 171.
- [20] J. G. Kovács, T. Tábi, *Polym. Eng. Sci.* 2011, 51, 843.
- [21] D. Karst, Y. Yang, *Polymer* 2006, 47, 4845.
- [22] H. Tsuji, *Polymer* 2000, 41, 3621.
- [23] G. Gorrasi, R. Pantani, in *Synthesis, Structure and Properties of Poly(lactic acid)*, Vol. 279 (Eds: M. L. Di Lorenzo, R.

- Androsch), Springer International Publishing, Cham **2018**, p. 119.
- [24] M. Shi, Q. Jiao, T. Yin, J. J. Vlassak, Z. Suo, *MRS Bull.* **2023**, 48, 45.
- [25] N. F. Zaaba, M. Jaafar, *Polym. Eng. Sci.* **2020**, 60, 2061.
- [26] H. Wang, X. Sun, P. Seib, *J. Appl. Polym. Sci.* **2003**, 90, 3683.
- [27] G. H. Yew, A. M. Mohd Yusof, Z. A. Mohd Ishak, U. S. Ishiaku, *Polym. Degrad. Stab.* **2005**, 90, 488.
- [28] M. Gáspár, Z. Benkó, G. Dogossy, K. Réczey, T. Czigány, *Polym. Degrad. Stab.* **2005**, 90, 563.
- [29] I. Danjaji, R. Nawang, U. Ishiaku, H. Ismail, Z. Mohd Ishak, *Polym. Test.* **2002**, 21, 75.
- [30] M. Hakkarainen, A.-C. Albertsson, S. Karlsson, *J. Appl. Polym. Sci.* **1997**, 66, 959.
- [31] M. A. Sawpan, K. L. Pickering, A. Fernyhough, *Composites, Part A* **2011**, 42, 310.
- [32] J. O. Akindoyo, M. D. Beg, S. Ghazali, H. P. Heim, M. Feldmann, *Composites, Part A* **2017**, 103, 96.
- [33] X. Ju, C. Grego, X. Zhang, *Bioresour. Technol.* **2013**, 144, 232.
- [34] C. Chaudemanche, P. Navard, *Cellulose* **2011**, 18, 1.
- [35] I. Eriksson, I. Haglind, O. Lidbrandt, L. Salmén, *Wood Sci. Technol.* **1991**, 25, 135.
- [36] G. I. Mantanis, R. A. Young, R. M. Rowell, *Cellulose* **1995**, 2, 1.
- [37] S. Mishra, J. B. Naik, Y. P. Patil, *Compos. Sci. Technol.* **2000**, 60, 1729.
- [38] R. Auras Ed., *Poly(lactic acid): Synthesis, structures, properties, processing, and applications*, Wiley-Blackwell, Oxford **2010**.
- [39] H. Tsuji, Y. Ikada, *J. Polym. Sci., Part A: Polym. Chem.* **1998**, 36, 59.
- [40] H. Tsuji, K. Ikarashi, *Polym. Degrad. Stab.* **2004**, 85, 647.
- [41] H. Tsuji, K. Ikarashi, *Biomaterials* **2004**, 25, 5449.
- [42] H. Tsuji, K. Ikarashi, *Biomacromolecules* **2004**, 5, 1021.
- [43] H. Tsuji, K. Nakahara, K. Ikarashi, *Macromol. Mater. Eng.* **2001**, 286, 398.
- [44] H. Tsuji, S. Miyauchi, *Polym. Degrad. Stab.* **2001**, 71, 415.
- [45] H. Tsuji, S. Miyauchi, *Polymer* **2001**, 42, 4463.
- [46] H. Tsuji, A. Mizuno, Y. Ikada, *J. Appl. Polym. Sci.* **2000**, 77, 1452.
- [47] D. Cam, S. H. Hyon, Y. Ikada, *Biomaterials* **1995**, 16, 833.
- [48] N. Gemmeke, M. Feldmann, H.-P. Heim, *Composites, Part A* **2019**, 118, 327.
- [49] C. Kahl, M. Feldmann, P. Sälzer, H.-P. Heim, *Composites, Part A* **2018**, 111, 54.
- [50] C. K. Falkenreck, N. Gemmeke, J.-C. Zarges, H.-P. Heim, *Polymers* **2023**, 15, 1606.
- [51] G. W. Ehrenstein, S. Pongratz, *Beständigkeit von Kunststoffen*, Hanser, München **2007**.
- [52] N. N. Hellman, T. F. Boesch, E. H. Melvin, *J. Am. Chem. Soc.* **1952**, 74, 348.
- [53] F. A. Schüll, Einfluss spezieller Eigenschaften der Stärke auf den Brauprozess, München **2012**.
- [54] R. Hampe, Synthese und Strukturcharakterisierung von neuartigen wasserlöslichen Stärkederivaten und Studien zu ihrer Verwendung in Dialyseprozessen, Jena **2018**.
- [55] A. M. Harris, E. C. Lee, *J. Appl. Polym. Sci.* **2010**, 115, 1380.

**How to cite this article:** V. Goetjes, J.-C. Zarges, H.-P. Heim, *J. Appl. Polym. Sci.* **2024**, 141(2), e54768. <https://doi.org/10.1002/app.54768>